Isolation and Characterization of a Proteinase K-Sensitive PrP^{Sc} Fraction†

Miguel A. Pastrana,‡ Gustavo Sajnani,‡ Bruce Onisko,§ Joaquín Castilla,|| Rodrigo Morales,|| Claudio Soto,|| and Jesús R. Requena*,‡

Prion Research Unit, Department of Medicine, School of Medicine, University of Santiago de Compostela, Rue de S. Francisco s/n, Santiago de Compostela, Galiza, Spain 15782, Western Regional Research Center, United States Department of Agriculture, Room 3124, 800 Buchanan Street, Albany, California 94710, and Department of Neurology, University of Texas Medical Branch, 301 University Boulevard, Galveston, Texas 77555

Received July 31, 2006; Revised Manuscript Received October 13, 2006

ABSTRACT: Recent studies have shown that a sizable fraction of PrP^{Sc} present in prion-infected tissues is, contrary to previous conceptions, sensitive to digestion by proteinase K (PK). This finding has important implications in the context of diagnosis of prion disease, as PK has been extensively used in attempts to distinguish between PrP^{Sc} and PrP^{C}. Even more importantly, PK-sensitive PrP^{Sc} ($sPrP^{Sc}$) might be essential to understand the process of conversion and aggregation of PrP^{C} leading to infectivity. We have isolated a fraction of $sPrP^{Sc}$. This material was obtained by differential centrifugation at an intermediate speed of Syrian hamster PrP^{Sc} obtained through a conventional procedure based on ultracentrifugation in the presence of detergents. PK-sensitive PrP^{Sc} is completely degraded under standard conditions (50 μg/mL of proteinase K at 37 °C for 1 h) and can also be digested with trypsin. Centrifugation in a sucrose gradient showed $sPrP^{Sc}$ to correspond to the lower molecular weight fractions of the continuous range of oligomers that constitute PrP^{Sc}. PK-sensitive PrP^{Sc} has the ability to convert PrP^{C} into protease-resistant PrP^{Sc}, as assessed by the protein misfolding cyclic amplification assay (PMCA). Limited proteolysis of $sPrP^{Sc}$ using trypsin allows for identification of regions that are particularly susceptible to digestion, i.e., are partially exposed and flexible; we have identified as such the regions around residues K110, R136, R151, K220, and R229. PK-sensitive PrP^{Sc} isolates should prove useful for structural studies to help understand fundamental issues of the molecular biology of PrP^{Sc} and in the quest to design tests to detect preclinical prion disease.

Since prions were defined as "proteinaceous infectious particles" and characterized as infectious agents composed almost exclusively of protein (*1*), substantial and diverse evidence has accumulated lending support to a stronger definition, according to which prions would be, in fact, infectious proteins (*2*−*5*). The prion protein, PrP,[1] is capable of adopting two basic conformations. Under the PrP^{C} form, it is a monomeric, glycosylated, α-helix-rich protein attached to cell membranes through a GPI anchor (*2*); in contrast, PrP^{Sc} appears as a β-sheet-rich, polymeric, insoluble molecule. PrP^{Sc} catalyzes the transformation of PrP^{C} into more PrP^{Sc} through a poorly characterized molecular mechanism (*2*, *3*, *6*). The structure of PrP^{Sc} is yet unknown, although several models have been proposed (*7*−*9*). These and future models need to conform to experimental constraints, such as those derived from electron micrographs of two-dimensional crystals of PrP^{Sc} (*7*, *10*) or chemical cross-linking studies (*11*).

Traditionally, in the absence of definitive conformation-specific antibodies, and without structural data, PrP^{Sc} has been defined operationally by means of two physicochemical characteristics that distinguish it from PrP^{C}: its resistance to proteinase K and its insolubility in detergents (*2*, *12*). Thus, treatment of a sample with 50 μg/mL PK for 1 h at 37 °C completely destroys PrP^{C}; in contrast, PrP^{Sc} is partially resistant to this treatment, resulting in cleavage of the amino terminal portion of this molecule, leaving a PK-resistant core termed PrP 27−30, 60−70 residues shorter than PrP^{Sc}. In the presence of detergent, PrP 27−30 forms characteristic rod-shaped structures readily visible by transmission electron microscopy (*13*). The amino terminal stretch of PrP^{C} spanning from the amino terminus to about position 121 is highly disordered, as surmised from NMR studies of recombinant PrP in solution, and it has been proposed that part of that stretch, up to the PK-cut position, is also disordered in PrP^{Sc}.

With regard to the second operational method to define PrP^{Sc}, insolubility in detergent, high-speed centrifugation under "standard conditions" (100000*g* for 1 h at 4 °C) allows pelleting PrP^{Sc}, leaving PrP^{C} in the supernatant (*12*). Resistance to PK and insolubility under "standard conditions", the two operational characteristics that define "*bona fide*" PrP^{Sc} (*12*), have been traditionally assumed to go hand in hand. Unexpectedly, more recent studies have revealed a more complex picture. Safar et al. first described the existence of a PK-sensitive fraction of PrP^{Sc} (*14*). These authors showed that denaturation with chaotropes enhances the immunoreactivity of PrP^{Sc} toward certain antibodies, a result of the uncovering of partially buried epitopes, which are equally available in native vs denatured PrP^{C} (*14*).

† This work was supported by research grants from the Spanish Ministry of Science and Technology (EET 2001-4861 to JRR) and the National Institutes of Health (NS049173 to CS).

* Corresponding author. Phone: +34-981-559904. Fax: +34-981-559904. E-mail: requenaj@usc.es.

‡ University of Santiago de Compostela.

§ United States Department of Agriculture.

|| University of Texas Medical Branch.

10.1021/bi0615442 CCC: $33.50
Published on Web 12/06/2006

Intriguingly, pretreatment of samples with PK considerably weakens the denaturation-dependent immunoreactivity enhancement effect, indicating the existence of a subset of PrP^{Sc} molecules that are completely degraded by PK and that were termed, in accordance, PK-sensitive PrP^{Sc} ($sPrP^{Sc}$). Subsequent studies by Tzaban et al. showed that, when brain and cell homogenates from scrapie-infected animals and cultures were subjected to sucrose gradients, PrP distributed in a continuum of aggregation sizes. Although PrP^{Sc} is present in the more dense fractions, corresponding to larger polymers, and was PK-resistant, PrP^{Sc} recovered from intermediate fractions, corresponding to smaller oligomers, was not (*12*). In contrast, homogenates from control brains or cell cultures only contained PrP in the very light fractions, corresponding to monomeric or at the most, dimeric PrP (*12*). These results suggest that PrP^{Sc} is a heterogeneous collection of oligomers of different sizes and that resistance to PK is dependent, at least in part, on its quaternary structure.

More recent studies highlight the importance of $sPrP^{Sc}$; in a recent study, as much as 80% of PrP^{Sc} in the brains of individuals who had died as a consequence of Creutzfeldt−Jakob disease (CJD) was estimated to be $sPrP^{Sc}$ (*15*). Because many methods rely on the use of PK to distinguish between PrP^{Sc} and PrP^{C} (*2*), a considerable underestimation of the amount of PrP^{Sc} present in samples might be expected. This would be of particular importance in the quest to develop analytical methods to detect minute amounts of PrP^{Sc} in biological fluids such as blood, which could constitute the basis of a preclinical prion test. Beyond this practical consideration, $sPrP^{Sc}$ might hold important clues on the structure of PrP^{Sc} and the process that leads to its generation and propagation.

We reasoned that, starting from a sample of PrP^{Sc} isolated through standard procedures that rely on ultracentrifugation in the presence of detergent, it would be possible to isolate a lighter fraction of smaller PrP^{Sc} oligomers that would remain in the supernatant at lower centrifugal forces. On the basis of Tzaban's results, we also reasoned that such smaller oligomers of PrP^{Sc} would be more sensitive to the effect of PK. Thus, by operationally adjusting our experimental conditions, one would possibly be able to obtain a fraction of $sPrP^{Sc}$. We describe here the isolation of such a fraction and its further characterization and introduce its possible use for structural studies.

EXPERIMENTAL PROCEDURES

Isolation of PrP^{Sc}. PrP^{Sc} was isolated from brains of terminally ill Syrian hamsters infected with the 263K strain of scrapie, using a slightly modified version of the procedure of Diringer et al. (*16*). This procedure involves low-speed centrifugation of a 10% brain homogenate in 10% sarkosyl to remove cell debris and centrifugation of the supernatant at high speed (g_{av} 149008*g*) through a sucrose cushion. The pellet is resuspended in 0.1% of Z-3,14 detergent (*N*-tetradecyl-*N*,*N*-dimethyl-3-ammonio-1-propanesulphonate, Boehringer Mannheim, Germany) and subjected to three additional cycles of pelleting at 149008*g* through sucrose cushions, followed by resuspension, first in this detergent, and later in deionized water at pH 8.5. Our modifications of the method consisted of inclusion of a cocktail of protease inhibitors (Complete, Roche Diagnostics, Penzberg, Germany) at a final concentration of 1X in all buffers used throughout the procedure up to the penultimate pellet, P145c, as defined in the mentioned study (*16*), which was resuspended, as described, in 20 mM Tris/HCl, pH 8.5 buffer (T8.5) not supplemented with the protease inhibitor cocktail. Also, treatment with PK of this fraction was omitted. The final pellet was resuspended in T8.5 containing 1% sarkosyl and no protease inhibitors at concentrations between 1 and 2 μg/μL by application of three to four 1 s pulses at an amplitude of 50% with a 4710 series probe ultrasonics homogenizer (Cole Parmer, Chicago, IL). The stock suspension thus prepared was frozen until further use; its purity was assessed by SDS-PAGE with Coomassie blue staining and MALDI and estimated to be approximately 80−85%. Several methods, all based on the same principle (pelleting in the presence of detergents) with minor variations in the number of centrifugation steps, centrifugation times, composition of buffers, etc., have been described to isolate PrP^{Sc} (*17*,*18*). Of note is that, when a control brain homogenate is subjected to the same procedure, no PrP is found in the pellets (Figure S1 in the Supporting Information and ref 17). Concentration of PrP^{Sc} was estimated by comparison of serial dilutions of this material with serial dilutions of a recombinant Syrian hamster, SHaPrP (90−231), standard, a generous gift of Giuseppe Legname, UCSF, on dot blots stained with Amido Black (*19*).

Isolation of $sPrP^{Sc}$. $sPrP^{Sc}$ was isolated from total PrP^{Sc} by ultracentrifugation at an intermediate speed. A 50−150 μL portion of the PrP^{Sc} stock suspension (see above) was homogenized by application of three to four sonication pulses of 1 s each, as described above, and spun in a TLX ultracentrifuge (Beckman, Fullerton, CA) using a TLA-120-1 rotor at 40 000 rpm (g_{av} 56806*g*) for 2 h at 20 °C. The supernatant, corresponding to $sPrP^{Sc}$ (see below), was collected, and the pellet was resuspended by brief sonication in a volume of T8.5 containing 1% sarkosyl equivalent to that of the supernatant. Fractions of supernatant and pellet were treated with 50 μg/mL PK at 37 °C for 1 h; the reaction was terminated with 2 M Pefabloc (Fluka, St. Louis, MO) and a fraction subjected to SDS-PAGE (*20*) and either stained with Coomassie blue or transferred to a PVDF membrane (Immobilon-P, Millipore, Billerica, MA) and analyzed by Western blotting using mAbs 3F4 (Dako, Glostrup, Denmark) or 6H4 (Prionics, Zurich, Switzerland) at 1:5000 and 1:2000 dilutions, respectively.

Conformation-Dependent Immunoreactivity. To measure the dependence of the immunoreactivity of $sPrP^{Sc}$ and $rPrP^{Sc}$ on protein denaturation, we used the dot blot procedure described by Serban et al. (*21*). Samples were diluted with deionized water to an approximate concentration of 12.5 ng/μL, and 2 μL of each sample was spotted on a dry nitrocellulose membrane. The dots were thoroughly air-dried. The membranes were then washed extensively with PBS

[1] Abbreviations: CB, conversion buffer (150 mM NaCl, 1% Triton X-100, 4 mM EDTA, complete 1X in PBS); CJD, Creutzfeldt−Jakob disease; GPI, glycosylinositol phospholipid; PBS, phosphate buffered saline; NBH, normal brain homogenate; PMCA, protein misfolding cyclic amplification; PK, proteinase K; PrP, prion protein; PrP^{C}, cellular prion protein isoform; PrP^{Sc}, scrapie prion protein isoform; $sPrP^{Sc}$, PK-sensitive PrP^{Sc}; $rPrP^{Sc}$, PK-resistant PrP^{Sc}; TIC, total ion current; TNS, 10 mM Tris, pH 7.5, 150 mM NaCl, 1% sarkosyl buffer; TSEs, transmisible spongiform encephalopathies; T8.5, 20mM Tris/HCl, pH 8.5 buffer; XIC, extracted ion chromatogram.

containing 0.3% Tween-20 and incubated for 10 min at room temperature in PBS with or without 4 M guanidinium hydrochloride; after thorough washing in PBS containing 0.3% Tween-20, the membrane was probed with mAb 3F4. Signal intensities were quantitated using the LabWorks 3.0 image analysis software (UVP, Cambridge, U.K.). Conformation dependence was calculated for each sample (N) as

$$Y(N) = I_{(N,0M)}/I_{(N,4M)}$$

where $I_{(N,0M)}/I_{(N,\ 4M)}$ are, respectively, blot signal intensities of a given sample with and without 4 M guanidine hydrochloride treatment.

Velocity Sedimentation in Sucrose Gradients. Samples of $sPrP^{Sc}$ or $rPrP^{Sc}$, ~2.5 μg, were diluted in 1.2 mL of 10 mM Tris, pH 7.5, 150 mM NaCl, and 1% sarkosyl (TNS) and loaded on top of 10−60% sucrose step gradients (*12*). Gradients were formed in polyallomer (11 × 34 mm) tubes from 600 μL of each of the following sucrose concentrations: 10, 15, 20, 25, 30, and 60% in water. The gradients were spun for 1 h at 4 °C at 50 000 rpm (g_{av} 200620*g*) in a MLS-50 rotor in a Biosafe Optima MAX ultracentrifuge (Beckman Coulter, Fullerton, CA). Twelve 300 μL fractions, following the load volume, were collected starting from the top of the tube; fraction 12 included the pellet.

PMCA. Different fractions obtained from the sucrose gradient sedimentation experiment were diluted with a minimal amount of conversion buffer (CB), consisting of PBS containing 150 mM NaCl, 1% Triton X-100, 4 mM EDTA, and Complete 1X to obtain samples of a similar PrP concentration, as determined by Western blot. These samples were serially diluted in NBH (10% normal brain homogenate) prepared in CB from 1/20 to 1/320 (final volume 100 μL). From each final dilution, 18 μL aliquots were immediately withdrawn and frozen at −80 °C (control samples); the remaining 82 μL portions were subjected to PMCA amplification (*22*−*24*) in 0.2 mL PCR polypropylene tubes (Fisher Scientific, Hampton, NH). Tubes were inserted in an adaptor and placed on the plate holder of a microsonicator (Misonix Model 3000, Farmingdale, NY); the plate was then placed in the water bath of the sonicator and incubated without shaking. The sonicator was programmed to perform incubation cycles of 30 min at 37 °C followed by a 20 s pulse of sonication at 60−80% potency for 48 h. Amplified and control samples were incubated with 50 μg/mL of PK for 60 min at 37 °C; the digestion reaction was stopped by addition of Laemmli electrophoresis buffer and boiling. Samples were subjected to SDS-PAGE and Western blotting, as described above. In parallel experiments, $sPrP^{Sc}$ was treated with PK or buffer for 60 min at 37 °C and then diluted in CB as appropriate and subjected to PMCA.

Limited Proteolysis. $sPrP^{Sc}$ (~3.5 μg) was treated with trypsin (Promega, Madison, WI) in T8.5 (final volume 10 μL) at 37 °C for 1 h at the indicated enzyme/substrate ratios (figure legends). SHaPrP (90−231), kept at −70 in 6M guanidine hydrochloride, was freshly refolded in 50 mM phosphate buffer, pH 7.4, extensively dialyzed against the same buffer, and treated with trypsin in a similar way. Reactions were stopped with Complete (Roche) and reaction mixtures analyzed by Western blot. Alternatively, samples were denatured by addition of solid guanidine hydrochloride to a final concentration of 6 M, acidified with 10% trifluoroacetic anhydride, and adsorbed to C-18 ZipTips (Millipore). Peptides were eluted according to the manufacturer's instructions and dried by centrifugal evaporation (SpeedVac, Savant, Farmingdale, NY). For analysis by nanospray LC/MS/MS, samples were redissolved in 40 μL of 6 M guanidine hydrochloride.

Nanospray LC/MS/MS. NanoLC−ESI−MS−MS was done with an Applied Biosystems (ABI/MDS Sciex, Toronto, Canada) model QStar Pulsar equipped with a Proxeon Biosystems (Odense, Denmark) nanoelectrospray source. Redissolved trypsin digests (20 μL) were loaded automatically onto a C-18 trap cartridge, and after washing, the trapped peptides were chromatographed on a reversed-phase column (Vydac 238EV5.07515, 75 μm × 150 mm; Hesperia, CA) fitted at the effluent end with a coated spray tip (FS360-50-5-CE, New Objective Inc., Woburn, MA). An LC Packings nanoflow LC system (Dionex, Sunnyvale, CA) with an autosampler, column switching device, loading pump, and nanoflow solvent delivery system was used to elute the column. Elution solvents were A (0.5% acetic acid in water) and B (80% acetonitrile, 0.5% acetic acid). Samples were eluted at 250 nL/min with the following gradient profile: 8% B at 0 min to 80% B in a 15 min linear gradient (held at 80% B for 5 min then back to 8% B for 10 min). The QStar Pulsar was externally calibrated daily and operated above a resolution of 7000. The acquisition cycle time of 6 s consisted of a single 1 s MS "survey" scan followed by a 5 s MS/MS scan. Ions between *m*/*z* 400 and 1000 of charge states between +2 and +5 having intensities greater than 40 counts in the survey scan were selected for fragmentation. The dynamic exclusion window was set to always exclude previously fragmented masses. A collision energy optimized for charge state and *m*/*z* was automatically selected by the Analyst QS 1.1 software after adjusting parameters to obtain satisfactory fragmentation of the Glu fibrinogen peptide (+2) and ACTH (+3 and +4). Nitrogen was used for the collision gas, and the pressure in the collision cell ranged from 3×10^{-6} to 6×10^{-6} Torr. The externally calibrated TOF−MS survey scans were processed with the "LCMS Reconstruct" tool in the Analyst software. The output is a list of peptide molecular weights calculated by deconvolution of multiple charge states and then identification of the monoisotopic ^{12}C species.

RESULTS

Isolation of an $sPrP^{Sc}$ Fraction. Centrifugation of a PrP^{Sc} suspension at an intermediate centrifugal force, as described in the Experimental Procedures, generated pellets and supernatants with divergent resistance to PK. Supernatants, typically making up 35−55% of the total starting PrP^{Sc} material, were much less resistant than pellets. By fine-tuning the centrifugal force and length of centrifugation, we were able to obtain a supernatant PrP^{Sc} fraction that was completely hydrolyzed by the standard treatment with PK at 50 μg/mL for 1 h at 37 °C ($sPrP^{Sc}$), as judged by Western blot using antibody 3F4 and Coomassie staining (Figure 1). Under the same conditions, an equivalent amount of the pellet produced the characteristic PK-resistant core (PrP 27−30) with an increased electrophoretic mobility, a consequence of the trimming of 65−70 amino terminal residues. We thereafter term this pellet fraction "$rPrP^{Sc}$". Treatment of $sPrP^{Sc}$ with lower concentrations of PK showed that this

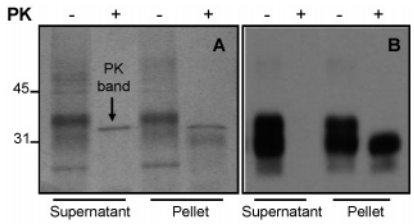

FIGURE 1: Isolation of a PK-sensitive PrP^{Sc} fraction: PrP^{Sc} was subjected to intermediate speed ultracentrifugation, as described in the Experimental Procedures, and supernatant and pellet fractions thus obtained subjected to PK treatment under standard conditions (50 μg/mL, 37 °C, 1 h) and analyzed by SDS-PAGE. A: Coomassie blue stain; B. Western Blot using mAb 3F4.

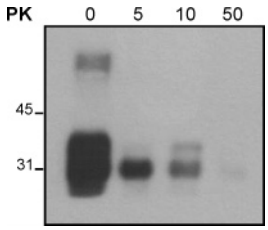

FIGURE 2: Partial PK resistance of $sPrP^{Sc}$. sPrPSc was treated with increasing concentrations of PK (μg/mL) at 37 °C for 1 h and analyzed by Western blot using mAb 3F4.

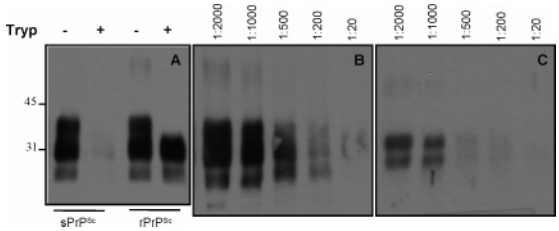

FIGURE 3: Susceptibility of $sPrP^{Sc}$ to trypsin digestion. Samples of $sPrP^{Sc}$ and $rPrP^{Sc}$ were treated with trypsin for 1 h at 37 °C and analyzed by Western blot. A: Equal amounts of $sPrP^{Sc}$ and $rPrP^{Sc}$ treated with a 1:60 enzyme/substrate ratio (mAb 3F4). B: Limited digestion of $sPrP^{Sc}$ with increasing trypsin/substrate ratios (mAb 3F4). C: Limited digestion of $sPrP^{Sc}$ (mAb 6H4).

material exhibits, as expected, some resistance to degradation by this enzyme (Figure 2).

We next studied susceptibility of $sPrP^{Sc}$ to trypsin. Treatment of $sPrP^{Sc}$ with trypsin at 37 °C for 1 h, at enzyme/substrate ratios in the range 1:20−1:60 (there was some variability with different substrate and trypsin batches) resulted in a virtually complete disappearance of the protein, as assessed by Western blot using antibody 3F4 (Figure 3A); under similar conditions, an equivalent amount of $rPrP^{Sc}$, treated with the same ratio of trypsin, yielded a band of approximately the same intensity as that of the untreated sample, albeit migrating slightly faster (Figure 3A). This apparent MW difference of 2000−3000 suggests clipping of $rPrP^{Sc}$ at arginines 37 and 48 in the putatively unstructured tail that, in contrast, is cleaved up to Gly90 by PK and agrees with previously published results relative to total PrP^{Sc} (*13*). Further experiments showed that decreasing trypsin/substrate ratios can be used to achieve limited proteolysis of $sPrP^{Sc}$ (Figure 3B). Western blots using mAb 6H4 (epitope 144−152) also showed a similar trypsin concentration-dependent signal disappearance (Figure 3C), suggestive of a generalized tryptic cleavage. When freshly refolded, recombinant SHaPrP-(90−231) was subjected to trypsin proteolysis under the same conditions, complete disappearance of the 3F4 signal was seen at an approximate enzyme/substrate ratio of 1:400, indicative of a much lower resistance to trypsin degradation.

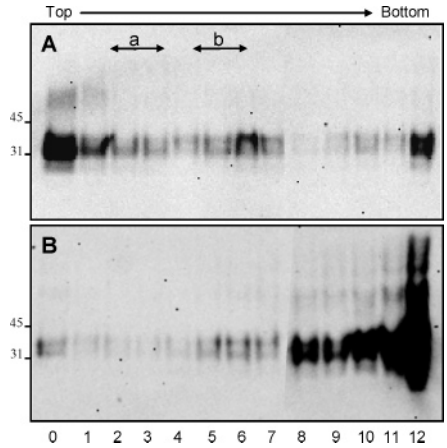

FIGURE 4: Size distribution of $sPrP^{Sc}$ (A) and $rPrP^{Sc}$ (B) in sucrose gradients. Equal amounts of $sPrP^{Sc}$ and $rPrP^{Sc}$ were loaded on the top of a preformed 10−60% step sucrose gradient; the gradient was spun for 1 h at 4 °C at g_{av} 200620*g*, fractions 0−12 collected from the top. Fractions were analyzed by Western blot using mAb 3F4. In parallel experiments under the same conditions, Apoferritin (443k) and Dextran Blue (2000k) emerged in the indicated fractions, a and b, respectively.

Biochemical Characterization of $sPrP^{Sc}$. When subjected to sucrose gradient centrifugation, $sPrP^{Sc}$ exhibited a distribution throughout the upper fractions, particularly 0−7 with a considerable amount of material present in fractions 0 (load volume) and 1 (Figure 4). Little material tailed in the lower fractions (*8*−*11*); some material was also recovered in the pellet fraction. When $rPrP^{Sc}$ was subjected to a similar treatment, its distribution showed, as expected, a pattern complementary to that of $sPrP^{Sc}$ with very little material present in early fractions (0−7) and most of it present in late fractions (8−12) including the pellet (Figure 4). It is known that lipid micelles can interfere with the mobility of proteins in sucrose gradients; therefore, we chose a concentration of 1% sarkosyl in our samples, which is known to prevent micelle formation (*25*). Furthermore, we conducted control experiments in which we took individual sucrose gradient fractions, dialyzed them against TNS, and reloaded the sample to a freshly prepared gradient. As seen in Figure S2, Supporting Information, such samples migrated to the same position as in the first separation experiment, which confirms these fractions contain oligomers of a defined size.

The molecular weight markers apoferritin (MW 443k) and Dextran Blue (MW 2000k), loaded on a gradient run in parallel under identical conditions, emerged in fractions ∼2 and ∼5, respectively (Figure 4). Extrapolation of these results would lead to the conclusion that, if an approximate MW of 35k is assigned to each PrP subunit, and assuming that the aggregates are entirely composed of PrP (*26*), the majority of $sPrP^{Sc}$ aggregates would be composed of aggregates of up to 12−15 PrP subunits, and most $rPrP^{Sc}$ would contain over 60 PrP subunits.

Different fractions obtained from the sucrose gradient centrifugation experiment were assayed for their converting capacity using the PMCA assay (*22*−*24*). More specifically, we assayed fractions 0 and (1 + 2) from $sPrP^{Sc}$, corresponding to very light and heavier fractions of $sPrP^{Sc}$, and fraction 11 from $rPrP^{Sc}$. As seen in Figure 5, when equal amounts of

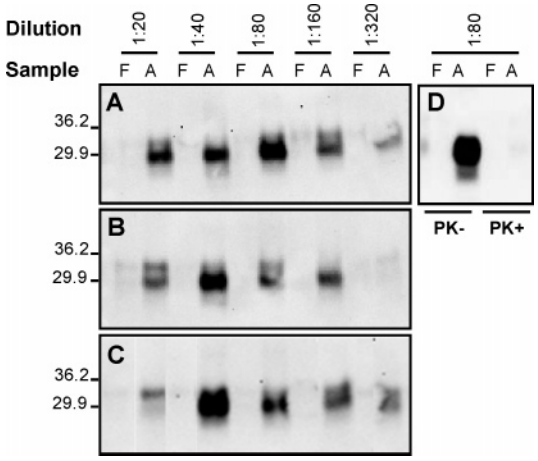

FIGURE 5: Transforming activity of $sPrP^{Sc}$ as shown by PMCA. Equivalent amounts of PrP^{Sc} from different fractions (A, fraction 0 from $sPrP^{Sc}$; B, combined fractions 1 + 2 from $sPrP^{Sc}$; C, fraction 11 from $rPrP^{Sc}$) obtained from the sucrose gradient sedimentation experiment were diluted in NBH and split in two samples, one frozen (F) and the other subjected to amplification by PMCA (A). After treatment with 50 μg/mL PK, samples were analyzed by Western blot (mAb 3F4). D: Aliquots of a $sPrP^{Sc}$ sample treated with or without PK at 37 °C for 1 h and subjected to PMCA.

PrP present in these fractions were subjected to PMCA, all three exhibited converting activity, surmised from the generation of PK-resistant PrP^{Sc} at the end of the PMCA cycles. In a control experiment, we compared the converting activity of $sPrP^{Sc}$ with or without prior treatment with PK and found that, as expected, PK-induced destruction of $sPrP^{Sc}$ abolished the converting activity (Figure 5D). It is of note that, in these experiments, the detection of PrP^{Sc} was done after PK treatment, which means that, in the case of $sPrP^{Sc}$ present in fractions 0 and (1 + 2), the conversion process progresses to generation of PK-resistant PrP^{Sc}. It remains to be studied what the ratio of $sPrP^{Sc}/rPrP^{Sc}$ produced by PMCA from the different fractions used is. Further dilutions of the samples, subjected to PMCA, were also conversion-competent. Given the high sensitivity of PMCA, it is not possible, from this experiment, to compare the relative efficacy of the different fractions tested, but it is clear that even the material obtained from fraction 0 is highly conversion-competent.

Further biochemical characterization of $sPrP^{Sc}$ was carried out using a version of the dot blot format CDI introduced by Serban et al. (*21*). As expected, treatment of total PrP^{Sc} blotted on a nitrocellulose membrane with 4 M guanidine, prior to probing with monoclonal antibody 3F4 resulted in a considerable increase in intensity (data not shown), in agreement with published results (*21*); $rPrP^{Sc}$ behaved also in a similar way, and for $sPrP^{Sc}$, guanidine treatment produced a significant yet lower enhancement of intensity (Figure 6).

Limited Proteolysis of $sPrP^{Sc}$. The fact that $sPrP^{Sc}$ can be digested by trypsin (Figure 3) prompted us to explore the possibility that $sPrP^{Sc}$ might be subjected to limited proteolysis experiments using this enzyme. This might allow for probing the susceptibility of individual lysine and arginine residues to cleavage, which in turn can provide some structural information. We digested $sPrP^{Sc}$ using trypsin to substrate ratios ranging from 1:2 to 1:2000 and analyzed the reaction mixtures by nanoLC−MS/MS. In agreement with

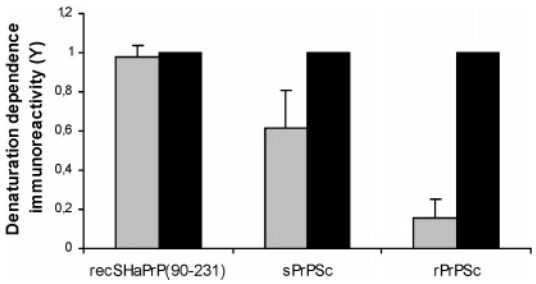

FIGURE 6: Denaturation dependent immunoreactivity of $sPrP^{Sc}$, $rPrP^{Sc}$, and recombinant SHaPrP (90−231). Samples were probed by dot blot (mAb 3F4) without (gray bars) or with (black bars) treatment with 4 M guanidinium hydrochloride. Y represents the ratio between signals obtained for a given sample without guanidinium hydrochloride treatment divided by signal obtained with 4 M guanidinium hycdrochloride; Y = 1 indicates a complete lack of conformation dependence. Data represent means and standard deviations (n = 4). Differences were statistically significant (student's t test) between recSHaPrP (90−231) and $sPrP^{Sc}$ ($p < 0.03$), recSHaPrP (90−231) and $rPrP^{Sc}$ ($p < 0.0001$), and $sPrP^{Sc}$ and $rPrP^{Sc}$ ($p < 0.02$).

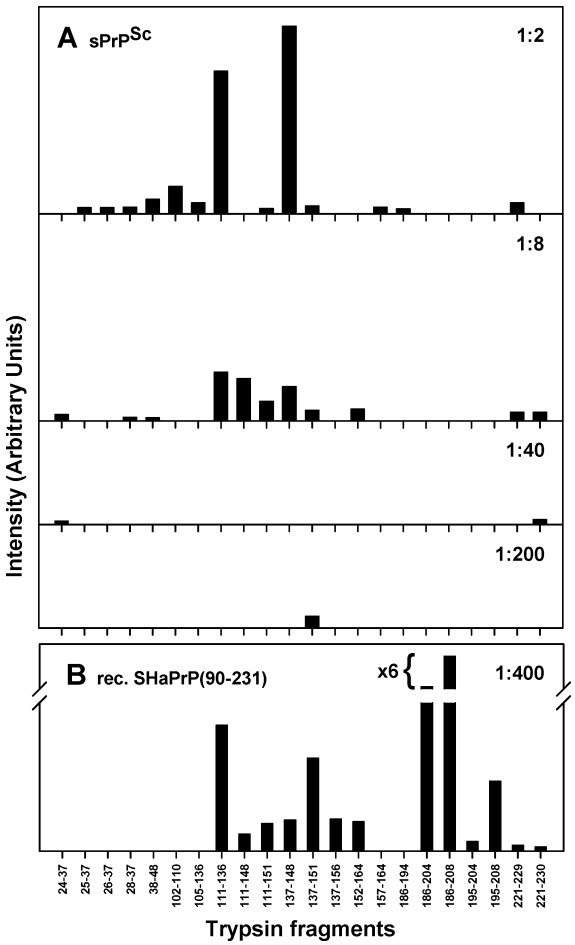

FIGURE 7: Tryptic fragments obtained by limited proteolysis of $sPrP^{Sc}$. Samples were treated with trypsin for 1 h at 37 °C at the indicated enzyme/substrate ratios. Tryptic fragments were identified by LC−MS, as described in the text. **A**: $sPrP^{Sc}$. **B**: recombinant SHaPrP (90−231). Bars represent relative peak areas in total intensity chromatograms (TIC) with all panels at the same scale, except as otherwise indicated. Data are representative of two independent experiments.

Western blot data (Figure 3), the lower enzyme/substrate ratios resulted in just a few detectable fragments (Figure 7). As expected, higher trypsin/substrate ratios resulted in detection of more fragments with overall higher intensities.

It is noteworthy that detection of a given fragment depends not only on cleavage of residues located at its boundaries but also on the intrinsic "detectability" of the resulting peptide; i.e., low MW peptides (<800) would not trigger MS−MS experiments, and others may suffer substantial losses during sample cleanup, etc. For PrP^{Sc}, glycosylation and the presence of the disulfide bond further limit the number of peptides that could be detected under our particular experimental conditions. With all this in mind, the most readily conspicuous fragments were 137−151, 24−37, and 221−230 (Figure 7 and Figures S3 and S4 in the Supporting Information). At higher concentrations of trypsin, besides these fragments, several others were detected, including 111−136, 137−148, 152−164, and 157−164. At an even higher trypsin concentration, intensity ratios of some fragments changed, indicating further fragmentation at previously intact internal residues. As an example, peptides 111−136 and 137−148, which do not have any intact internal K or R residues, increased steadily as the trypsin concentration increased, whereas fragments 111−148, 111−151, and 152−164 exhibited a bimodal behavior, with maximum relative intensities at intermediate trypsin concentrations.

DISCUSSION

There is a growing interest in PK−sensitive PrP^{Sc}, a previously unnoticed PrP^{Sc} fraction. There are several reasons for this: on one hand, recent studies suggest that, in many instances, $sPrP^{Sc}$ makes up a very sizable fraction of total PrP^{Sc} (*15*); on the other hand, $sPrP^{Sc}$ might offer explanations for some puzzling experimental results that have been difficult to accommodate within the current prion paradigm, such as reports of disease transmission in the absence of "PK-resistant PrP" (*27*), or the inherent difficulty to propagate some prions, such as those causing some genetic forms of disease (*28*). Finally, the existence of $sPrP^{Sc}$ has clear practical implications, as it limits the usefulness of analytical techniques relying on the use of PK to detect PrP^{Sc}. This should be carefully considered in the development of the urgently needed ultrasensitive tests capable of detecting PrP^{Sc} in preclinical disease-suffering subjects and animals. Furthermore, the possibility of missing infected specimens containing a high proportion of $sPrP^{Sc}$ becomes an issue with obvious health implications.

We report here a simple method to isolate a PK-sensitive fraction of PrP^{Sc}. It is evident that our definition of $sPrP^{Sc}$ is operational: we have chosen a specific combination of centrifugal force and centrifugation time that allows for isolation of a fraction of PrP^{Sc} that will, precisely, be completely degraded under the standard, yet arbitrary, conditions defined by treatment by 50 μg/mL PK at 37 °C for 1 h. However, it is also evident that modifying the parameters of centrifugation allows one to obtain an alternative fraction that would meet the definition of $sPrP^{Sc}$, were different operational PK-treatment parameters to be chosen. Our results show, in agreement with the work of Tzaban et al. (*12*), that PK resistance of PrP^{Sc} shows a strong dependence on the quaternary structure of PrP^{Sc}. Indeed, PrP^{Sc} isolated following a standard procedure based on ultracentrifugation in the presence of detergents is a collection of oligomers with a continuum of sizes (Figure 4). Our results confirm that larger PrP^{Sc} polymers exhibit higher PK resistance than smaller ones.

Resistance to digestion by PK is a function of accessibility to the enzyme, and larger oligomers offer the possibility of enhanced protection of certain PrP subunits. Because there is not a definitive model of PrP^{Sc}, it is difficult to envision how such enhanced protection is achieved. In contrast to PrP 27−30, obtained by proteolytic treatment of PrP^{Sc} in the presence of detergent, and organized in rods of measurable dimensions (*2*, *13*), there are no available experimental data on the organization or shape of PrP^{Sc} oligomers. The most parsimonious view would be that PrP^{Sc} and PrP 27−30 share basic structural features, such as the way in which PrP subunits are stacked (*7*) and that clipping by PK of the very labile, random coil amino termini leads to further packing. Such a possibility is compatible with a mechanism of PrP^{Sc} growth and transmission based on nucleated polymerization. In this model, the β-sheet domains of a PrP subunit, whatever their specific organization might be (β-helices, simple parallel β-sheets, etc.; *7*,*8*), act as templates or scaffolds for the next PrP subunit (*6*, *29*). The alternative possibility is that PrP^{Sc} and PrP 27−30 have unrelated quaternary structures and that PrP 27−30, with its proposed regular stacking, is formed totally *de novo* through a complete rearrangement of the subunits that constitute the PrP^{Sc} aggregate; in that case, PrP^{Sc} oligomers might even be formed by featureless aggregates. However, it is more difficult in that case to envision how one β-sheet rich PrP^{Sc} subunit might influence a PrP^{C} molecule to adopt a PrP^{Sc} conformation. In any case, it seems obvious that, whether well-structured stacks or random aggregates, the larger PrP^{Sc} oligomers become more protected from PK digestion.

A property of PrP^{Sc} that also shows, in our hands, a significant dependence on size is conformation-dependent immunoreactivity. With regard to this, $sPrP^{Sc}$ exhibited a distinct enhancement of immunoreactivity after guanidine hydrochloride treatment (Figure 6); however, such enhancement was significantly lower than that of $rPrP^{Sc}$, made up, as discussed, of larger polymers. This is in agreement with Tzaban et al. (*12*), who showed a decrease in conformational-dependent immunoreactivity in the lighter fractions of brain homogenates subjected to sucrose gradient fractionation.

Our results confirm that $sPrP^{Sc}$ is able to convert PrP^{C} into PrP^{Sc}. Fractions of PrP^{Sc} comprising oligomers of small relative size were as effective as larger polymers to convert PrP^{C} into PrP^{Sc} in the PMCA assay. This result strongly suggests that $sPrP^{Sc}$ is indeed *bona fide* PrP^{Sc} and not an off-route molecular species along the pathway that leads from PrP^{C} to a putative "full-fledged" PrP^{Sc} (*14*). Studies aimed at determining whether $sPrP^{Sc}$ is infectious and what the kinetics of its accumulation *in vivo* look like are in process. A recent study showed that the most infectious fraction of solubilized PrP 27−30 corresponds to relatively small oligomers comprising 14−28 PrP molecules; smaller and larger aggregates show reduced specific infectivity and, beyond certain given size thresholds, are not infectious at all (*30*). *In vitro* converting capacity also peaked at the same intermediate size. Even though extreme caution must be exercised when comparing results obtained with PrP^{Sc} and those obtained with MW markers, our data suggest that the material present in our loading fraction (fraction 0, Figure 4) corresponds to oligomers with very low molecular weights; a direct interpolation would suggest that they contain less than 12 PrP subunits. Thus, our data suggest that even

such low molecular weight oligomers are capable of initiating prion replication.

The susceptibility of $sPrP^{Sc}$ to virtually complete degradation by trypsin opens the possibility of using limited proteolysis as a tool to probe its structure. This approach has been successfully used to obtain structural information on a variety of proteins that were not amenable to other techniques (*31*−*33*). Lysine and arginine residues that are accessible (solvent-exposed) and do not participate in strong ionic interactions are more easily cleaved by trypsin. The results described in Figure 7 constitute an example of the applicability of this strategy to PrP^{Sc}. Thus, comparison of yields of specific cleavage products obtained from $sPrP^{Sc}$ and recombinant PrP after application of increasing amounts of trypsin allows one to conclude that residues R136, R151, K220, and R229 are particularly susceptible to cleavage in $sPrP^{Sc}$. Other residues, such as K110, R148, R156, R164, K185, and K194 are partially cleaved as well, but this requires larger amounts of trypsin. In contrast, evidence of cleavage of all these residues in recombinant SHaPrP (90−231) is seen even at the lowest concentration of trypsin tested (trypsin/substrate ratio of 1:400). A similar analysis of the $rPrP^{Sc}$ showed an overall pattern that was very similar to that of $sPrP^{Sc}$, although with much lower yields of peptide fragments (data not shown). In a recent model of mouse PrP 27−30 based on a left-handed β-helical core (*7*), residue R150, equivalent to hamster R151, is located in a loop protruding from the central β-helical core, which would be in good agreement with accessibility of this residue; residues K219 and R228, equivalent to hamster K220 and R229, are located in the carboxy-terminal α-helix, again, allowing good accessibility, provided there is no hindrance from carbohydrates attached to PrP^{Sc} in the carboxy-terminal region. However, R135, equivalent to hamster R136, is placed in the middle of the β-helical assembly, a location that theoretically would not facilitate access of trypsin. It should be noted that an exhaustive analysis of cleavage patterns is complicated by the fact that in PrP^{Sc} several of the possible products are glycosylated, which renders them impossible to detect with the methods used. Additional and more extensive studies, including time course experiments, will provide structural information that, together with data obtained with other techniques, such as chemical cross-linking (*11*) and surface labeling studies, will allow testing of the structural models proposed thus far and the design of new models that can explain the physicochemical data obtained.

To summarize, we have developed an easy method to isolate a PK-sensitive fraction of PrP^{Sc}. A first survey of the biochemical properties of this material, composed by a light fraction of PrP^{Sc} oligomers, shows that it has prion-converting activity and that it is susceptible to digestion by specific proteolytic enzymes, such as trypsin. This material should prove useful to study fundamental aspects of the biochemistry of PrP^{Sc}.

ACKNOWLEDGMENT

We are grateful to Emilio Nogueira from the Department of Physiology, University of Santiago de Compostela, for outstanding technical advice. We also thank Alejandro Brun and José A. Rodríguez from the CISA, Madrid, for help with hamster inoculations.

SUPPORTING INFORMATION AVAILABLE

Figures showing the presence of PrP in supernatants and pellets of a healthy hamster brain homogenate subjected to the PrP^{Sc} isolation procedure, consistent location of PrP^{Sc} fractions in sucrose gradient sedimentation, examples of an extracted ion chromatogram (XIC), and an MS/MS spectrum corresponding to a tryptic peptide of $sPrP^{Sc}$. This material is available free of charge via the Internet at http://pubs.acs.org.

REFERENCES

1. Prusiner, S. B. (1982) Novel proteinaceous infectious particles cause scrapie, *Science 216*, 136−144.
2. Prusiner, S. B. (1998) Prions, *Proc. Natl. Acad. Sci. U.S.A. 95*, 13363−23383.
3. Soto, C., and Castilla, J. (2004) The controversial protein-only hypothesis of prion propagation, *Nat. Med. Suppl. 7*, S63−67.
4. Legname, G., Baskakov, I. V., Nguyen, H. O., Riesner, D., Cohen, F. E., DeArmond, S. J., and Prusiner, S. B. (2004) Synthetic mammalian prions, *Science 305*, 673−676.
5. Castilla, J., Saa, P., Hetz, C., and Soto, C. (2005) In vitro generation of infectious scrapie prions, *Cell 121*, 195−206.
6. Caughey, B. (2003) Prion protein conversions: insight into mechanisms, TSE transmission barriers and strains, *Br. Med. Bull. 66*, 109−120.
7. Govaerts, C., Wille, H., Prusiner, S. B., and Cohen, F. E. (2004) Evidence for assembly of prions with left-handed beta-helices into trimers, *Proc. Natl. Acad. Sci. U.S.A. 101*, 8342−8347.
8. DeMarco, M. L., and Daggett, V. (2004) From conversion to aggregation: protofibril formation of the prion protein, *Proc. Natl. Acad. Sci. U.S.A. 10*, 12293−12298.
9. Stork, M., Giese, A., Kretzschmar, H. A., and Tavan, P. (2005) Molecular dynamics simulations indicate a possible role of parallel beta-helices in seeded aggregation of poly-Gln, *Biophys. J. 88*, 2442−2451.
10. Wille, H., Michelitsch, M. D., Guénebaut, V., Supattapone, S., Serban, A., Cohen, F. E., Agard, D. A., and Prusiner, S. B. (2002) Structural studies of the scrapie prion protein by electron crystallography, *Proc. Natl. Acad. Sci. U.S.A. 99*, 3563−3568.
11. Onisko, B., Fernandez, E. G., Freire, M. L., Schwarz, A., Baier, M., Camiña, F., Garcia, J. R., Rodriguez-Segade Villamarin, S., and Requena, J. R. (2005) Probing PrP^{Sc} structure using chemical cross-linking and mass spectrometry: evidence of the proximity of Gly90 amino termini in the PrP 27-30 aggregate, *Biochemistry 44*, 10100−10109.
12. Tzaban, S., Friedlander, G., Schonberger, O., Horonchilk, L., Yedidia, Y., Shaked, G., Gabizon, R., and Taraboulos, A. (2002) Protease-sensitive scrapie prion protein in aggregates of heterogeneous sizes, *Biochemistry 41*, 12868−12875.
13. McKinley, M. P., Meyer, R. K., Kenaga, L., Rahbar, F., Cotter, R., Serban, A., and Prusiner, S. B. (1991) Scrapie prion rod formation in vitro requires both detergent extraction and limited proteolysis, *J. Virol. 65*, 1340−1351.
14. Safar, J., Wille, H., Itrri, V., Groth, D., Serban, H., Torchia, M., Cohen, F. E., and Prusiner, S. B. (1998) Eight prion strains have PrP^{Sc} molecules with different conformations, *Nat. Med. 4*, 1157−1165.
15. Safar, J. G., Geschwind, M. D., Deering, C., Didorenko, S., Sattavat, M., Sanchez, H., Serban, A., Vey, M., Baron, H., Giles, K., Miller, B. L., DeArmond, S. J., and Prusiner, S. B. (2005) Diagnosis of human prion disease, *Proc. Natl. Acad. Sci. U.S.A. 102*, 3501−3506.
16. Diringer, H., Beekes, M., Özel, M., Simon, D., Queck, I., Cardone, F., Pocchiari, M., and Ironside, J. W. (1997) Highly infectious purified preparations of disease-specific amyloid of transmissible spongiform encephalophathies are not devoid of nucleic acids of viral size, *Intervirology 40*, 238−246.
17. Bolton, D. C., Bendheim, P. E., Marmorenstein, A. D., and Potempska, A. (1987) Isolation and structural studies of the intact scrapie agent protein, *Arch. Biochem. Biophys. 258*, 579−590.

18. Caughey, B., Raymond, G. J., Priola, S. A., Kocisko, D. A., Race, R. E., Bessen, R. A., Lansbury, P. T., Jr., and Chesebro, B. (1999) Methods for studying prion protein (PrP) metabolism and the formation of protease-resistant PrP in cell culture and cell-free systems, *Mol. Biotechnol. 13*, 45−55.
19. Beekes, M., Baldauf, E., Cassens, S., Diringer, H., Keyes, P., Scott, A. C., Wells, G. A. H., Brown, P., Gibbs, C. J., Jr., and Gajdusek, D. C. (1995) Western blot mapping of disease-specific amyloid in various animal species and humans with transmissible spongiform encephalopathies using a high-yield purification method, *J. Gen. Virol.* 76, 2567−2576.
20. Laemmli, U. K. (1970) Cleavage of structural proteins during the assembly of the head of bacteriophage T4, *Nature 227*, 680−685.
21. Serban, D., Taraboulos, A., DeArmond, S. J., and Prusiner, S. B. (1990) Rapid detection of Creutzfeldt-Jakob disease and scrapie prion proteins, *Neurology 40*, 110−117.
22. Saborio, G. P., Permanne, B., and Soto, C. (2001) Sensitive detection of pathological prion protein by cyclic amplification of protein misfolding, *Nature 411*, 810−813.
23. Castilla, J., Saá, P., and Soto, C. (2004) Cyclic Amplification of Prion Protein Misfolding, in: *Techniques in Prion Research* (Lehman, S., and Grassi, J., Eds.), pp 198-213, Birkhouser, Basel.
24. Saá, P., Castilla, J., and Soto, C. (2004). Cyclic Amplification of Prion Protein Misfolding, in *Amyloid Proteins: Methods and Protocol.* (Sigurdsson, E. M., Ed.) pp 53−65, Humana Press, Totowa, NJ.
25. Riesner, D., Kellings, K., Post, K., Wille, H., Serban, A., Groth, D., Baldwin, M. A., and Prusine, r S. B. (1996). Disruption of prion rods generates 10-nm spherical particles having high α-helical content and lacking scrapie infectivity, *J. Virol. 70*, 1714−1722.
26. Chiesa, R., Piccardo, P., Quaglio, E., Drisaldi, B., Si-Hoe, S. L., Takao, M., Ghetti, B., and Harris, D. A. (2003) Molecular distinction between pathogenic and infectious properties of the prion protein, *J. Virol. 77*, 7611−7622.
27. Lasmezas, C. I., Deslys, J. P., Robain, O., Jaegly, A., Beringue, V., Peyrin, J. M., Fournier, J. G., Hauw, J. J., Rossier, J., and Dormont, D. (1997) Transmission of the BSE agent to mice in the absence of detectable abnormal prion protein, *Science 275*, 402−405.
28. Brown, P., Gibbs, C. J., Rodgers-Johnson, P., Asher, D. M., Sulima, M. P., Bacote, A., Goldfarb, L. G., and Gajdusek, D. C. (1994) Human spongiform encephalopathy: the National Institutes of Health series of 300 cases of experimentally transmitted disease, *Ann. Neurol. 35*, 513−529.
29. Come, J. H., Fraser, P. E., and Lansbury, P. T., Jr. (1993) A kinetic model for amyloid formation in the prion diseases: Importance of seeding, *Proc. Natl. Acad. Sci. U.S.A. 90*, 5959−5963.
30. Silveira, J. R., Raymond, G. J., Hughson, A. G., Race, R. E., Sim, V. L., Hayes, S. F., and Caughey, B. (2005) The most infectious prion protein particles, *Nature 437*, 257−261.
31. Hubbard, S. J. (1998) The structural aspects of limited proteolysis of native proteins, *Biochim. Biophys. Acta 1382*, 191−206.
32. Kheterpal, I., Williams, A., Murphy, C., Bledsoe, B., and Wetzel, R. (2001) Structural features of the Aβ amyloid fibril elucidated by limited proteolysis, *Biochemistry 40*, 11757−11767.
33. Neurath, H. (1980) Limited Proteolysis, Protein Folding and Physiological Regulation, in *Protein Folding* (Jaenicke, R., Ed.) pp 501−523, Elsevier, Amsterdam, The Netherlands.

BI0615442